The sodium leak channel NALCN encodes the major background sodium ion conductance in mouse anterior pituitary cells

Marziyeh Belal[1&2*], Mariusz Mucha[1], Arnaud Monteil[4], Paul G Winyard[5], Robert Pawlak[1], Jamie J. Walker[6,7&8], Joel Tabak[1*], Mino D C Belle[1&3*]

[1] University of Exeter Medical School, Hatherly Labs, Streatham Campus, Prince of Wales Road, Exeter, Devon, UK.

[2] Northwestern University, Feinberg School of Medicine, Chicago, IL 60611, United States.

[3] Division of Neuroscience and Experimental Psychology, School of Biological Sciences, Faculty of Biology, Medicine and Health, The University of Manchester, Manchester, UK

[4] IGF, University of Montpellier, CNRS, INSERM, Montpellier, France.

[5] University of Exeter Medical School, St Luke's Campus, Exeter EX1 2LU

[6] College of Engineering, Mathematics and Physical Sciences, University of Exeter, Exeter, UK.

[7] EPSRC Centre for Predictive Modelling in Healthcare, University of Exeter, Exeter, UK.

[8] Bristol Medical School, Translational Health Sciences, University of Bristol, Bristol, UK.

***Corresponding Authors:** mino.belle@machester.ac.uk, marziyeh.belal@northwestern.edu and j.tabak@exeter.ac.uk

Author Contributions: M.B, M.M, A.M, P.G.W, R.P, J.J.W, J.T and M.D.C.B conceived and designed research; M.B and M.M performed genetic manipulation experiments and M.B performed electrophysiology experiments as well as calcium imaging and data analysis; M.B, A.M, J.J.W, J.T and M.D.C.B wrote the paper.

Competing Interest Statement: The authors declare no competing interests.

Keywords: Background sodium channel, nonselective cationic conductance, sodium leak channels, NALCN, pituitary cells, endocrine cells, electrical activity

This file includes:
Main Text
Figures 1 to 6

Abstract

The pituitary gland produces and secretes a variety of hormones that are essential to life, such as for the regulation of growth and development, metabolism, reproduction, and the stress response. This is achieved through an intricate signalling interplay between the brain and peripheral feedback signals that shapes pituitary cell excitability by regulating ion channel properties of these cells. In addition, endocrine anterior pituitary cells fire action potentials spontaneously to regulate intracellular calcium ($[Ca^{2+}]_i$) level, an essential signalling conduit for hormonal secretion. To this end, pituitary cells have to critically regulate their resting membrane potential (RMP) close to firing threshold, but the molecular identity of the ionic mechanisms involved remains largely unknown. Here, we revealed that the sodium leak channel NALCN, known to modulate neuronal excitability elsewhere in the brain, acts to regulate excitability in the mouse anterior endocrine pituitary cells. Using viral transduction combined with powerful electrophysiology methods and calcium imaging, we show that NALCN forms the major Na^+ leak conductance in these cells, appropriately tuning cellular RMP for sustaining spontaneous firing activity. Genetic interruption of NALCN channel activity drastically hyperpolarised the cells, suppressing firing and ($[Ca^{2+}]_i$) oscillations. Remarkably, we uncover that NALCN conductance formed a very small fraction of the total cell conductance, but yet had a profound impact on pituitary cell excitability. Our results also provide a possible mechanism through which hypothalamic and hormone feedback signals can powerfully affect pituitary activity to influence hormonal function.

Introduction

The electrical activity of excitable cells appropriately responds to signals that are externally driven and/or those that are intrinsically derived to support essential physiological functions, such as breathing, heartbeat, and hormone release (Cui et al, 2016; Protze et al, 2017; Rorsman and Ashcroft, 2018; Bertram et al, 2018). Such excitability capacity relies on depolarising conductances that appropriately maintain the resting membrane potential (RMP) of cells near their firing threshold to support the spontaneous discharge of action potentials (APs). In hormone-secreting cells of the anterior pituitary gland, spontaneous AP firing results in rhythmic Ca^{2+} entry through voltage-gated calcium channels. These cytosolic/intracellular calcium ($[Ca^{2+}]_i$) oscillations serve a plethora of key physiological purposes, such as maintaining Ca^{2+} levels in intracellular calcium stores, regulating gene expression as well as evoking hormonal secretion (Mollard & Schlegel, 1996; Kwiecien & Hammond, 1998; Stojilkovic, 2012). Indeed, the silencing of spontaneous firing in endocrine pituitary cells abolishes $[Ca^{2+}]_i$ oscillations and hormone secretion (Kucka et al, 2010).

The ability for pituitary cells to produce spontaneous APs is in part due to the maintenance of their depolarised RMP relative to the much-hyperpolarised K^+ equilibrium potential (Fletcher et al, 2018). Replacing extracellular Na^+ with large impermeable cations, such as $NMDG^+$, starves the cells to Na^+ entry, suppressing the cell's ability to depolarise. Indeed, such treatments hyperpolarises the RMP, abolishing firing activity and $[Ca^{2+}]_i$ oscillations (Simasko, 1994; Sankaranarayan & Simasko, 1996; Kwiecien and Hammond, 1998; Tsaneva-Atanasova et al, 2007; Kucka et al, 2010, 2012; Tomic et al, 2011; Liang et al, 2011; Zemkova et al, 2016; Kayano et al, 2019). This indicates that constitutively active inward-depolarising Na^+-dependent currents/conductance in pituitary cells critically operates to maintenance of the RMP close to the firing threshold. Pharmacological and electrophysiological investigation of this inward leak current suggested it to be mediated by a TTX-insensitive, voltage-independent, and constitutively active Na^+-permeable channel/conductance (Fletcher et al, 2018). However, the molecular identity of the channels responsible for such resting Na^+ conductance in pituitary cells remains unknown.

The voltage-independent nonselective Na^+ leak channel NALCN has emerged as the major background Na^+-dependent conductance in several neuronal populations. For example, NALCN is essential for maintaining spontaneous AP firing in hippocampal neurons (Lu et al, 2007), GABAergic and dopaminergic neurons of the midbrain (Lutas et al, 2016; Philippart and Khaliq, 2018) and neurons of the suprachiasmatic nucleus (Flourakis et al, 2015). In the ventral respiratory neurons of the brain stem, NALCN activity facilitates rhythmic and carbon dioxide-stimulated breathing, as well as responsiveness to neuropeptides (Lu et al, 2007; Shi et al, 2016; Yeh et al, 2017), and NALCN regulate excitability in endocrine cells, such as pancreatic β cells (Swayne et al, 2009).

In the pituitary, a high level of NALCN mRNA expression is reported (Swayne et al, 2009); recent transcriptomic data also indicate that anterior pituitary cells express the NALCN gene and its known regulatory subunits (UNC-79, UNC-80, FAM155A) at level that is significantly higher when compared with gene expression of other known cationic leak channels, such as the TRP and HCN channels (Paul Le Tissier, Jacques Drouin and Patrice Mollard, personal communication, 04/2021). In addition, the pharmacological profile of NALCN in neurons is similar to that of resting Na^+ conductance measured in pituitary cells: TTX-insensitive, extracellular Ca^{2+}- and $NMDG^+$- sensitive (Fletcher et al, 2018; Lu et al, 2007), and recent work has indicated that NALCN activity influences excitability in GH3 pituitary clonal cell line (Impheng et al, 2021).

Together, this strongly suggests that NALCN is the primary contributor to the background Na^+ conductance and $[Ca^{2+}]_i$ oscillations in anterior endocrine pituitary cells, and consequently plays a key role in regulating pituitary cell excitability. To evaluate this, we used a parallel lentiviral-mediated NALCN knockdown strategy combined with powerful electrophysiology methods and calcium imaging in mouse primary anterior pituitary cells. Our results unequivocally revealed that NALCN is the main contributor to the background Na^+-dependant depolarising conductance in pituitary cells, which action is key to maintain cellular excitability. Remarkably, we were also able to estimate the magnitude of this NALCN conductance.

Results

NALCN channel protein is expressed in primary mouse anterior pituitary cells

Previous research has revealed the expression of the *Nalcn* gene in mouse anterior pituitary gland at the mRNA level (Swayne et al, 2009). Thus, we first confirmed NALCN protein expression in mouse primary endocrine pituitary cells with a NALCN antibody directed against the extracellular epitope of the NALCN channel protein (Alomone Labs, Israel, #ASC-022). Our results revealed the presence of NALCN channel in mouse endocrine anterior pituitary cells (Figure 1), with the majority of the anterior pituitary cells stained for NALCN. No staining was observed when the NALCN antibody was omitted (Figure 1H).

Figure 1

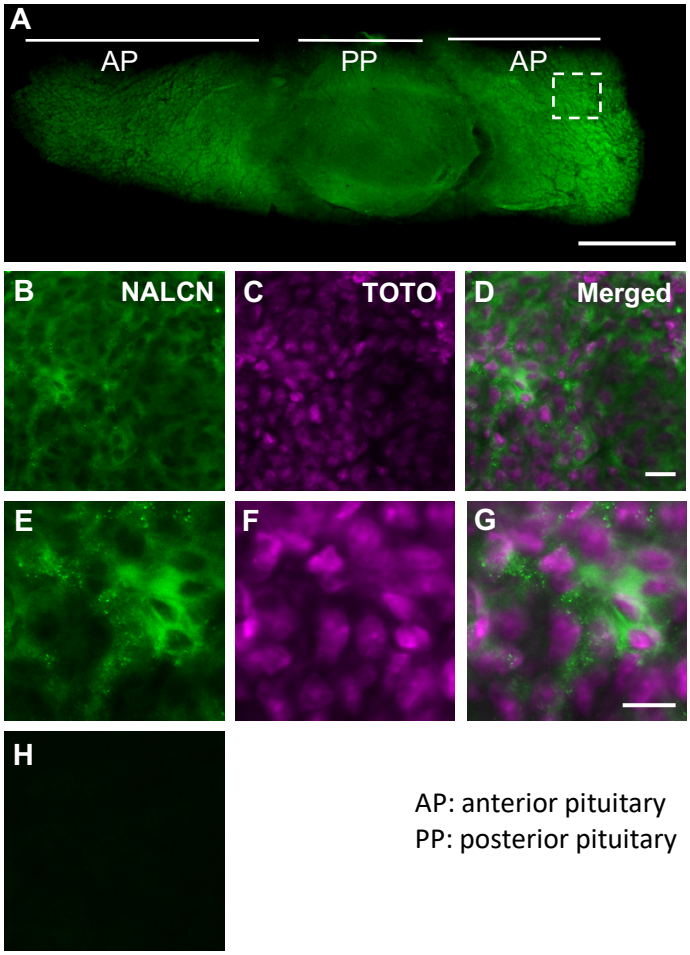

Figure 1. The mouse pituitary gland expresses NALCN ion channel. Immunofluorescence staining revealed the presence of NALCN channel protein in the mouse anterior pituitary gland (n=3). NALCN channel is shown in green. TOTO-3 (shown in magenta) was used to identify cell bodies by visualising cellular nucleic acids. **A)** Transverse section of a pituitary gland under 10X magnification excited with 488 nm light to detect NALCN channel immunofluorescence. **B)** NALCN channel visualisation in the area defined by dashed square in A. **C)** TOTO-labelled nucleic acid in the same area shown in B. **D)** Merged image from B and C. **B**, **C** and **D** are under 20X magnification. **E-G)** are under higher digital magnification using confocal microscopy. **H)** Negative control tissue for which the primary anti-NALCN antibody was omitted showing a lack of staining. Scale bars indicate 500 μm in panel A, and 20 μm in panels D and G.

NALCN regulates spontaneous firing in primary pituitary cells

Although gadolinium (Gd^{3+}) and flufenamic acid (FFA) act to suppress spontaneous firing in pituitary cells by causing hyperpolarisation (Kucka et al, 2012), and thus revealing the presence of a functional non-selective cationic conductance (NSCC) in these cells, it is noteworthy that Gd^{3+} and FFA are not specific blockers for a particular non-selective

cationic conductance. Thus, NSCCs other than NALCN may contribute to the effects of FFA and Gd^{3+} on membrane potential and firing activity. To determine if NALCN is the main NSCC in endocrine anterior pituitary cells, we used a genetic manipulation approach to directly and selectively alter the activity of NALCN, investigating its role in the regulation of membrane potential and spontaneous firing in these cells. To this end, we used a lentiviral-mediated knockdown strategy to decrease NALCN channel expression/activity level in mouse endocrine pituitary cells (see methods), and then evaluated the resulting changes in electrophysiological properties of these cells.

Our data revealed that most, if not all, untreated control (untreated Ctrl) and scramble control (SCR Ctrl) cells exhibited spontaneous firing activity (Figure 2A, B, D, F), consistent with previous reports (*reviewed in* Fletcher et al, 2018). In contrast, 90% (28 of 31) of NALCN knockdown (NALCN KD) cells were found to be silent (Figure 2C, D, F), compared to just 17% (5 of 30) in SCR control and 19% (6 of 31) in untreated control cells (Figure 2D, F). In addition, NALCN KD cells exhibited a significantly more hyperpolarised resting membrane potential (RMP) compared both to untreated and SCR Ctrl cells (NALCN KD RMP: -63.6 ± 8.5 mV (mean ± SD), n=31, 12 animals; SCR Ctrl: -45.2 mV ± 5.8 mV, n=30, 12 animals; untreated Ctrl: -47.5 mV ± 7.8, n=31, 12 animals; $p<0.001$, one-way ANOVA with post hoc Bonferroni correction; Figure 2E). There was no significant difference between the SCR Ctrl and untreated Ctrl cells, for neither the firing frequency (untreated Ctrl: 0.7 ± 0.6 Hz, n=25; SCR Ctrl: 0.5 ± 0.4 Hz, n=25, $p>0.1$, *t*-test; Figure 2F) nor the RMP (untreated Ctrl: -47.6 ± 7.6 mV, n=31; SCR Ctrl: -45.2 mV ± 5.8 mV, n=30 $p>0.1$, *t*-test; Figure 2E). Our results, therefore, indicate that NALCN activity in pituitary cells is critical for maintaining firing activity and sustaining of cellular RMP. In addition, since our results strongly indicated that the viral transduction *per se* did not affect the firing activity or RMP of pituitary cells, we henceforth made comparisons between NALCN KD and SCR Ctrl cells only.

Figure 2

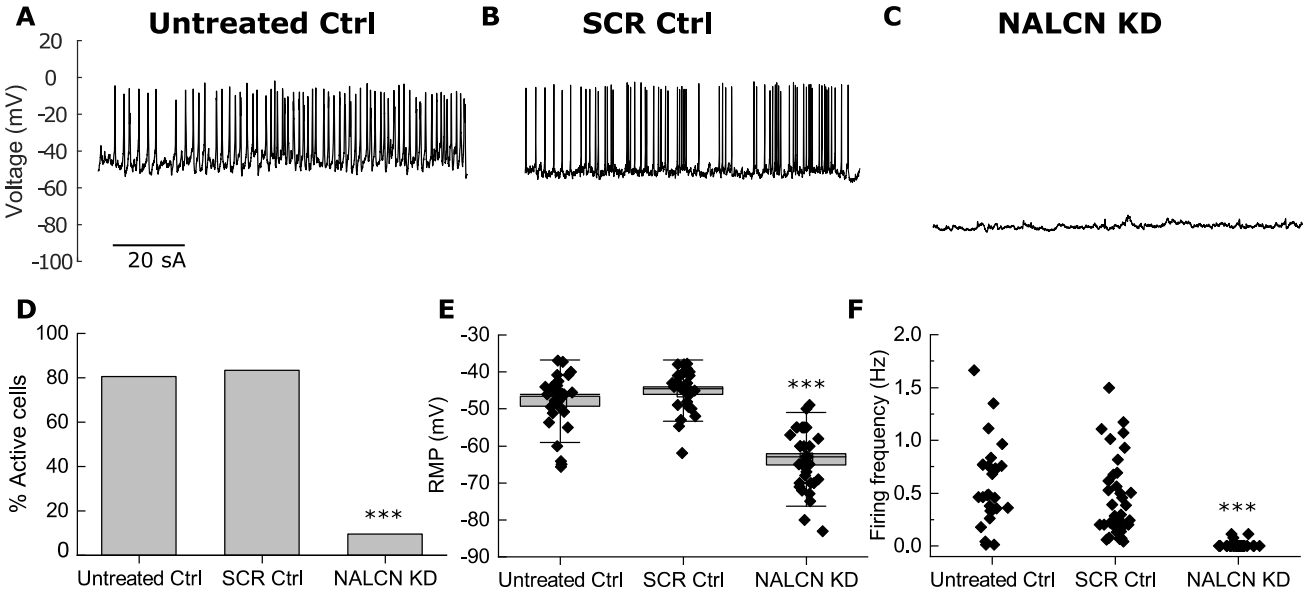

Figure 2. Knock-down of NALCN silences electrical activity in mouse pituitary cells. Representative traces of spontaneous firing activity from **A)** an untreated and **B)** a scramble control (SCR Ctrl) pituitary cell. **C)** Representative trace of electrical activity in a NALCN knockdown (NALCN KD) pituitary cell. **D)** Percentages of active and silent cells in untreated control, SCR Ctrl, and NALCN KD pituitary cells. **E)** Resting membrane potential of untreated control, SCR Ctrl, and NALCN KD pituitary cells (data presented as mean ± SD, untreated control: -47.6 ± 7.6 mV, n=31 vs SCR Ctrl: -45 mV ± 5.8 mV, n=30, p>0.1; NALCN KD: -63.6 ± 8.5 mV, n=31 vs SCR Ctrl and untreated control, p < 0.001, one-way ANOVA with Bonferroni correction). **F)** Distribution of firing frequency between untreated Ctrl, SCR Ctrl, and NALCN KD cells over a course of 600 seconds (data presented as mean ± SD, NALCN KD: 0 Hz, n= 31 vs SCR Ctrl: 0.5 ± 0.4 Hz, n= 25 and vs untreated Ctrl: 0.7 ± 0.6 Hz, n= 25, p < 0.001; SCR Ctrl vs untreated Ctrl: p > 0.1, one-way ANOVA with Bonferroni correction). Only 3/31 NALCN KD cells fired action potential, albeit at a lower frequency (0.1 ± 0.02 Hz) relative to the untreated and SCR controls. *** represents p < 0.001. In **(E)** boxes and whiskers represent the standard error of the mean and standard deviation , respectively. Each black dotes in **(E)** and **(F)** shows values from individual cells.

Small conductance injection restores firing in NALCN KD primary pituitary cells

Having rendered pituitary cells hyperpolarised-silent with NALCN KD, we next used dynamic-clamp to examine whether the injection of nonselective cationic conductance to these silent NALCN KD cells could restore RMP and spontaneous firing activity. Indeed, hyperpolarised-silent NALCN KD cells became depolarised and restored typical firing activity and frequency when the non-selective cationic conductance was injected by very

small amounts, such as 0.02 nS (Figure 3A). The added conductance required to bring NALCN KD cells to the typical RMP and firing activity/frequency observed in SCR Ctrl cells ranged from 0.02 to 0.12 nS (median 0.05 nS, n=28, Figure 3B).

Taken together, this first set of results indicate that NALCN is a key player in pituitary cell excitability, by modulating the RMP and subsequently, firing activity in primary pituitary cells. The amount of NALCN conductance lost by the cells after NALCN KD, as determined by dynamic clamp, was estimated to be on the order of 0.05 nS.

Figure 3

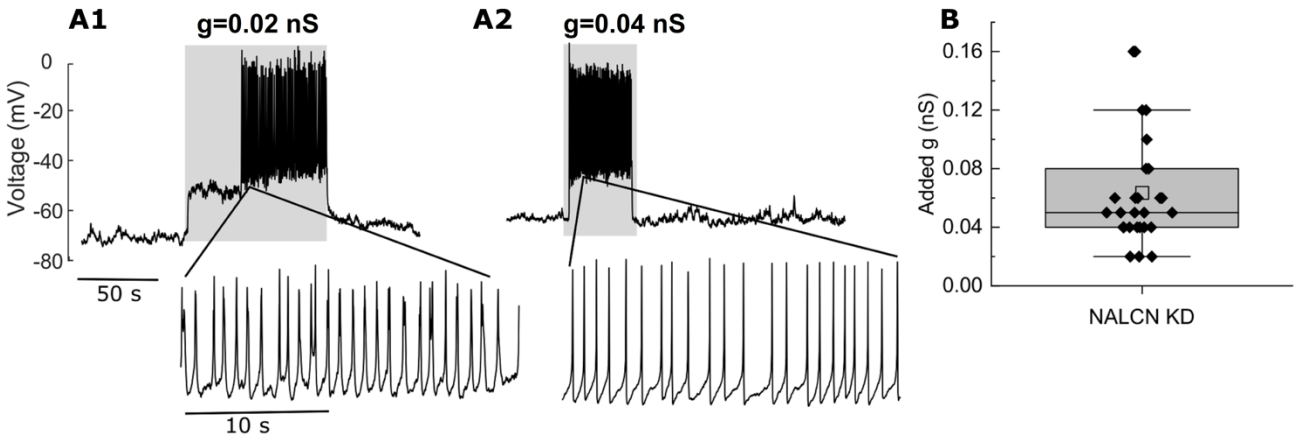

Figure 3. Dynamic clamp addition of nonselective cationic conductance restores firing activity in silent NALCN KD pituitary cells. A) Two representative voltage traces of silent NALCN KD pituitary cells. Firing activity was restored once the nonselective cationic conductance (g) was increased by amount as minute as 0.02 nS (e.g. silent cells depolarised and discharged barrages of action potentials when 0.02 or 0.04 nS conductance was applied (grey box), immediately returning to baseline after termination of added conductance. **B)** The distribution of added conductance (g) values required for restoring firing activity in hyperpolarised-silent NALCN KD pituitary cells. Median: 0.05 nS, n=28 from 12 animals.

NALCN majorly contributes to the inward Na^+ leak currents in primary pituitary cells

To further determine the contribution of the NALCN-mediated inward leak current over other background Na^+ currents in pituitary cells, we compared the inward current density in SCR Ctrl and NALCN KD cells while maintaining them at a holding potential of -80 mV, which in our setup also minimises any influence of K^+ channel conductance. At -80 mV, the holding current density was significantly larger in the SCR Ctrl group compared to NALCN KD group (Figure 4A-C, SCR Ctrl (mean ± SD): -0.72 ± 0.2 pA/pF, n=15, 8

animals; NALCN KD: -0.19 ± 0.13 pA/pF, n=16, 8 animals; p< 0.001, *t*-test), confirming that the NALCN KD cells were indeed more hyperpolarised than their SCR Ctrl counterparts. Remarkably, this background Na^+ conductance was reduced by 0.045 nS in SCR Ctrl, but by only 0.015 nS in NALCN KD (3 times smaller than what is measured in SCR Ctrl) when extracellular Na^+ was substituted by the Na^+ channel impermeant cation $NMDG^+$. This indicates that the measured inward currents in SCR Ctrl were being mediated by a background Na^+ conductance that was nearly absent in NALCN KD cells (Figure 4D, SCR Ctrl (median ± interquartile): 0.045 ± 0.02 nS, n = 16; vs NALCN KD: 0.015 ± 0.01 nS, n = 15; 8 animals in each condition, p < 0.001, Mann Whitney test).

These findings indicate that NALCN indeed contributes to most of the inward leak conductance in pituitary cells. Our results also provide a rough estimate of NALCN conductance magnitude in pituitary cells, by noting that the difference in background Na^+ conductance between SCR Ctrl and NALCN KD cells is 0.03 nS (0.045 nS – 0.015 nS). This is probably an underestimate since some residual NALCN conductance may still be available in NALCN KD cells following the lentiviral knockdown. Importantly, our results identify that a change in background Na^+ conductance of near 0.03 nS was enough to profoundly silence the electrical activity of endocrine anterior pituitary cell. This finding is consistent with endocrine pituitary cells having very large input resistance (~5 GΩ; Oxford and Dubinsky, 1988), meaning, very small variation in the current results in drastic changes in the RMP. This also agrees with our dynamic clamp observation where a 0.05 nS inward leak conductance injection was sufficient at fully restoring RMP and firing activity in NALCN KD cells (see above section and compare Figures 3 with 4).

Figure 4

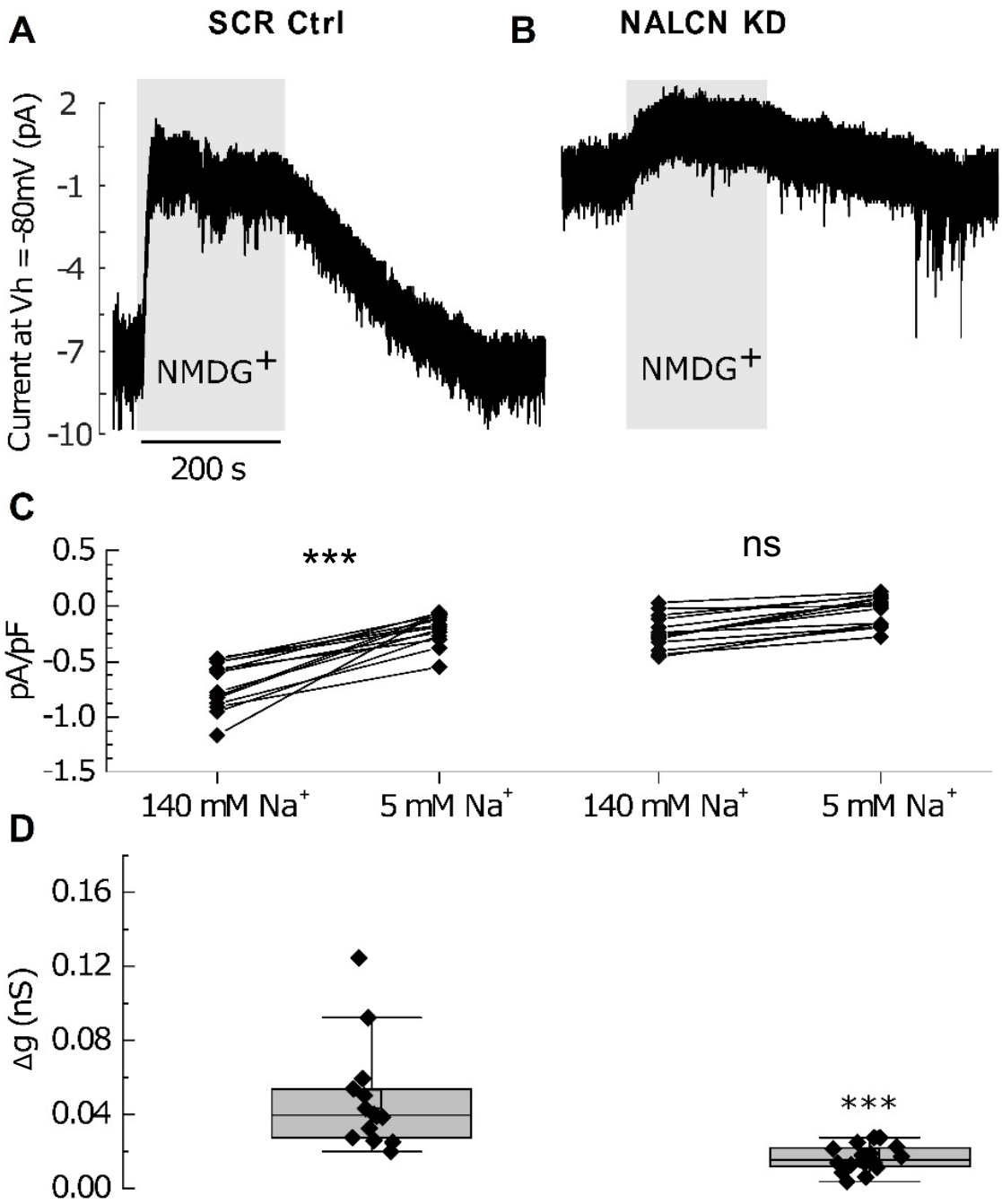

Figure 4. NALCN contributes to most of the inward Na^+ leak conductance in endocrine anterior pituitary cells. A-B) Representative traces of inward Na^+ leak currents (V_h = -80 mV) in a SCR Ctrl and NALCN KD pituitary cells as revealed by the substitution of extracellular Na^+ with $NMDG^+$ (grey boxes). **C)** The density of the inward Na^+ leak current in NALCN KD cells was significantly reduced compared to SCR Ctrl (data presented as ∆mean ± SD, SCR Ctrl: -0.72 ± 0.2 pA/pF (-5.2 ± 1.9 pA), n=15; NALCN KD: -0.19 ± 0.13 pA/pF (-1.5 ± 0.9 pA), n=16; 8 animals per condition, $p < 0.001$, *t*-test). **D)** Extracellular Na^+ substitution with $NMDG^+$ caused significant loss of

370 background Na^+ conductance in control but not in NALCN KD cells (data represented as
371 ΔMedian ± interquartile, SCR control: 0.045 ± 0.02 nS, n = 16; NALCN KD: 0.015 ± 0.01
372 nS , n = 15; p < 0.001, Mann Whitney test).
373
374 **NALCN is required for spontaneous intracellular Ca^{2+} oscillations in primary**
375 **pituitary cells**
376 Previous studies have shown that the pattern of spontaneous firing determines the
377 amplitude and duration of $[Ca^{2+}]_i$ oscillations in anterior endocrine pituitary cells
378 (Stojilkovic et al, 2005, Stojilkovic et al, 2012), a necessary signalling link with excitability
379 for hormonal secretion. Thus, we next tested whether NALCN KD affects spontaneous
380 $[Ca^{2+}]_i$, oscillations in these cells. We found that approximately 57% (51/90) of SCR Ctrl
381 pituitary cells exhibited spontaneous $[Ca^{2+}]_i$, oscillations (Figure 5A). In contrast, only
382 11% (4/36) of NALCN KD cells displayed such $[Ca^{2+}]_i$, transients (Figure 5), while the
383 remaining 89% (32/36) were quiescent and did not generate any $[Ca^{2+}]_i$, oscillations
384 (Figure 5B). The percentage (57%) of pituitary cells that produced $[Ca^{2+}]_i$, oscillations in
385 Ctrl conditions was consistent with previous reports (Tomić et al, 2011). To quantitatively
386 compare the size of the $[Ca^{2+}]_i$, oscillations between the SCR Ctrl and NALCN KD cells,
387 the standard deviation (SD) of the baseline Ca^{2+} ratio trace for each individual cell was
388 calculated over 600 seconds. Here, we use the size of the SD as a measure of the $[Ca^{2+}]_i$,
389 oscillations/fluctuations magnitude (for example compare Figure 5A and B). Comparing
390 the SD between the two groups revealed a significant difference between SCR Ctrl and
391 NALCN KD cells (Figure 5C, SCR Ctrl: median=0.04, n=90; NALCN KD: median=0.015,
392 n=36; p<0.001, Mann Whitney test, 5 animals per condition with each animal providing
393 roughly equal number of cells), with $[Ca^{2+}]_i$, ratios showing larger fluctuations in SCR
394 Ctrl cells when compared with NALCN KD cells. Together, this indicated that NALCN
395 plays a key role in regulating $[Ca^{2+}]_i$, oscillations in primary pituitary cells. As in SCR Ctrl
396 cells, challenging NALCN KD cells with high extracellular K^+ (15 mM) induced
397 depolarisation and consequently a rise in $[Ca^{2+}]_i$, ratios, serving as a positive control for
398 these cells.
399
400
401
402
403
404
405
406
407

408 **Figure 5**

409 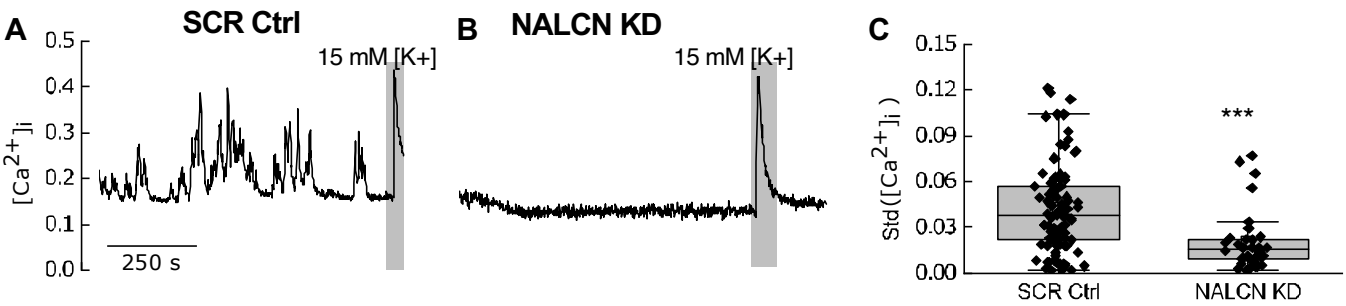

415

416 **Figure 5. NALCN KD impacts intracellular Ca^{2+} transients.**

417 **A)** Representative trace of intracellular Ca^{2+} ($[Ca^{2+}]_i$) oscillations in an SCR control (SCR
418 Ctrl) pituitary cell. **B)** A representative trace of $[Ca^{2+}]_i$ in a NALCN KD pituitary cell,
419 showing abolished $[Ca^{2+}]_i$ oscillations. **C)** The standard deviation (Std) of each $[Ca^{2+}]_i$
420 ratio trace was calculated and statistical analysis revealed a significant alteration of
421 $[Ca^{2+}]_i$ oscillations between the two groups (SCR Ctrl: median= 0.04, n = 90; NALCN KD:
422 median= 0.015, n = 36, 5 mice per condition, $p < 0.001$, Mann Whitney test). Box: inter-
423 quartile, Whiskers: range, excluding outliers, Central line: median. The last responses in
424 panels A and B (grey boxes) represent $[Ca^{2+}]_i$ response to a rise in extracellular K^+ (15
425 mM), used here as positive control to report cell viability.

426

427 **NALCN mediates a low extracellular Ca^{2+}-induced depolarisation in primary**
428 **pituitary cells**

429 Removal of extracellular Ca^{2+} ($[Ca^{2+}]_e$) activates a low and sustained excitatory inward
430 leak current in hippocampal neurons (Chu et al, 2003), by a mechanism that directly
431 involves NALCN, acting through the UNC80-NALCN complex to regulate excitability (Lu
432 et al, 2010). It is reported that in primary anterior pituitary cells, lowering or elimination
433 of $[Ca^{2+}]_e$ evoked similar effects on cellular excitability, causing severe membrane
434 depolarisation and silencing of firing, presumably through depolarisation blockade
435 (Stojilkovic, 2006; Sankaranarayanan and Simasko, 1996; Kwiecien and Hammond,
436 1998; Tsaneva-Atanasova et al, 2007). This raises the possibility that, as in hippocampal
437 neurons, NALCN could be responsible for the low $[Ca^{2+}]_e$-induced depolarisation in the
438 pituitary, providing us with yet another opportunity to functionally identify NALCN in
439 pituitary cells. We test this by assessing the effects of reducing $[Ca^{2+}]_e$ on pituitary cells
440 excitability.

441

442 Consistent with previous studies in neurons, lowering of $[Ca^{2+}]_e$ (from 2 to 0.1 mM)
443 caused a significant increase in inward leak current in SCR Ctrl pituitary cells (median ±
444 interquartile: −0.8 ± 0.6 pA/pF to −1.5 ± 0.5 pA/pF, n = 15; $p < 0.001$, Kruskal-Wallis,
445 Figure 6A,C, 6 animals). Subsequent replacement of extracellular Na^+ with $NMDG^+$

reduced the holding current (from −1.5 ± 0.5 pA/pF to −0.3 ± 0.2 pA/pF, n = 15, $p < 0.001$, Kruskal-Wallis, Figure 6A, C), indicating that the $[Ca^{2+}]_e$ -induced depolarisation is Na^+ mediated. Lowering $[Ca^{2+}]_e$ in NALCN KD pituitary cells produced a rise in inward leak current (from −0.37 ± 0.35 pA/pF to −0.5 ± 0.25 pA/pF, n = 13, $p < 0.05$, Figure 6B, C). However, in contrast, this rise in inward leak current in NALCN KD cells was substantially reduced in comparison with measurements in Ctrl cells (median of Δcurrent-density ± interquartile in SCR Ctrl: −0.6 ± 0.6 pA/pF, n = 13, NALCN KD: −0.13 ± 0.1 pA/pF, n = 13, from 6 mice, $p < 0.001$, Mann Whitney test, Figure 6D). This indeed indicates that similarly to what is observed in hippocampal neurons, NALCN is involved in pituitary cell sensitivity to reduced extracellular Ca^{2+}, and strongly suggest being the mechanism involved in the low Ca^{2+}-induced depolarisation observed in pituitary cells.

Figure 6

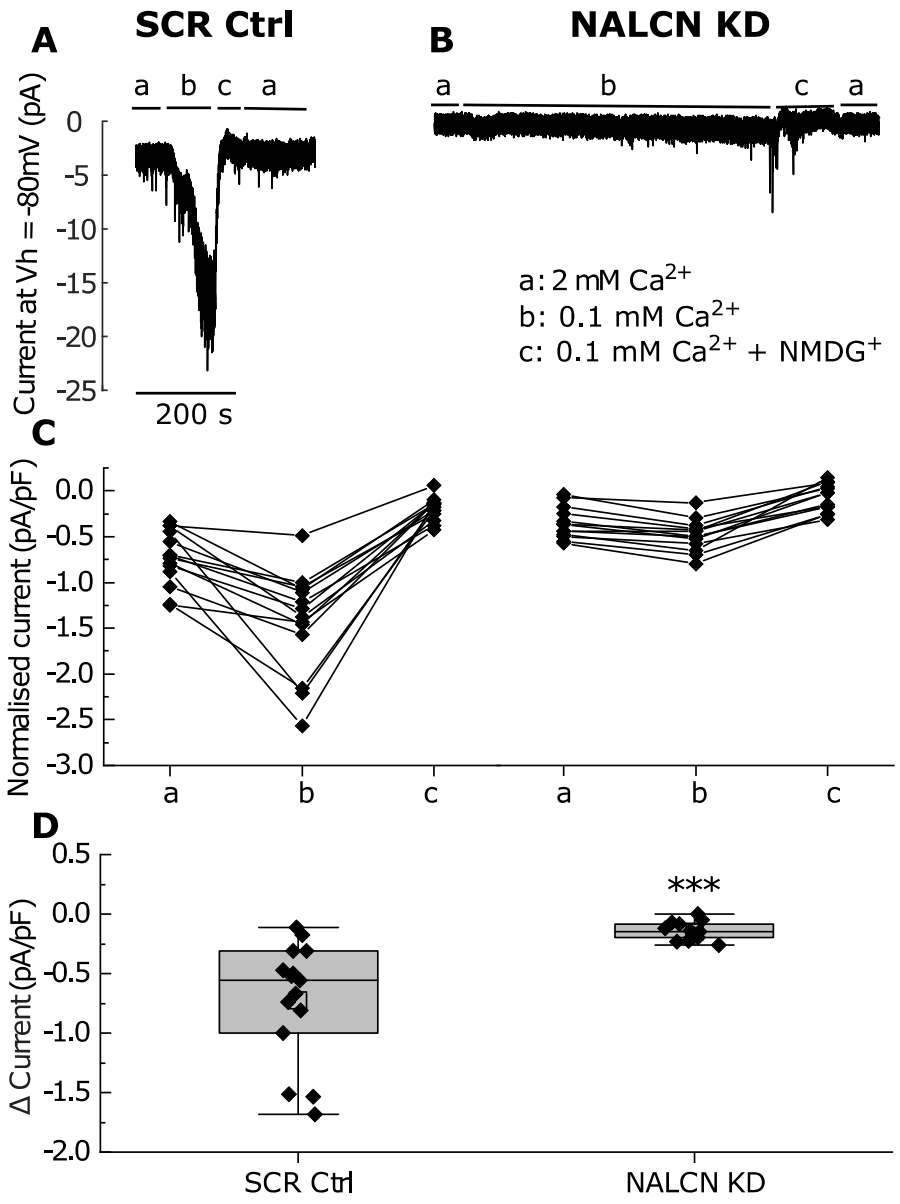

483 **Figure 6. NALCN is sensitive to changes in extracellular Ca^{2+} level**. **A-B)**
484 Representative traces of inward leak current in SCR control (SCR Ctrl) and NALCN KD
485 pituitary cells. From baseline conditions (a), reducing extracellular Ca^{2+} level evoked an
486 inward leak current in SCR Ctrl but not in NALCN KD pituitary cells (b). Subsequent
487 replacement of extracellular Na^{+} with $NMDG^{+}$ in reduced extracellular Ca^{2+} returned the
488 inward leak current back to near baseline level (c and a). In **B)** Representative trace of
489 the inward leak current in a NALCN KD pituitary cell; lowering the extracellular Ca^{2+}
490 resulted in a small rise in the inward leak current. Notice that we maintained NALCN KD
491 pituitary cells in low extracellular Ca^{2+} for longer period of time (>200 s) to rule out any
492 further changes in current during application. **C)** Normalised inward leak current in 2mM
493 Ca^{2+} (a), 0.1 mM Ca^{2+} (b), and 0.1 mM Ca^{2+} + $NMDG^{+}$ (c) in SCR Ctrl (left) and NALCN
494 KD (right) cells. **D)** The overall rise in inward leak current after reducing extracellular Ca^{2+}
495 in SCR Ctrl (left) compared to NALCN KD cells (right). ∆Median ± interquartile in SCR
496 Ctrl: −0.6 ± 0.6 pA/pF, n = 13; NALCN KD: −0.13 ± 0.1 pA/pF, n = 13, from 6 animals, p
497 < 0.001, Mann Whitney test. Box: inter-quartile, Whiskers: range excluding outliers,
498 Central line: median.
499
500 **Discussion**
501 We have used a lentiviral-mediated knockdown approach combined with powerful
502 electrophysiology methods and calcium imaging to provide the first compelling evidence
503 that NALCN forms the dominant depolarising conductance in anterior endocrine pituitary
504 cells. Our approach revealed that NALCN channel activity is critical at regulating the
505 electrical and $[Ca^{2+}]_i$ activity of these cells.
506
507 **NALCN regulates the excitability of mouse anterior pituitary cells**
508 Irrespective of cell-types, spontaneous firing in anterior pituitary cells is crucial to
509 maintain normal physiological functions, such as hormone secretion, gene expression
510 and intracellular Ca^{2+} ($[Ca^{2+}]_i$) oscillations (Kwiecien and Hammond, 1998; Stojilkovic et
511 al, 2010; Fletcher et al, 2018). However, the molecular identity of the major non-selective
512 cationic channels (NSCC) that critically enables spontaneous firing in these cells remains
513 unresolved (Fletcher et al, 2018). Nevertheless, pharmacological studies have revealed
514 that NSCCs are unequivocally Na^{+}-dependent and tetrodotoxin (TTX)-
515 resistant/insensitive (Simasko, 1994; Sankaranarayanan and Simasko, 1996; Kucka et
516 al, 2010; Liang et al, 2011; Tomic et al, 2011; Zemkova et al, 2016). Studies using RNA
517 expression profile and non-selective pharmacological manipulations have suggested
518 that transient receptor cation channels (TRPC), as well as hyperpolarisation-activated
519 cyclic nucleotide-gated channel (HCN) may also contribute to the NSCC described in
520 pituitary cells and related cell lines (Tomic et al, 2011; Kucka et al, 2012; Kayano et al,

521 2019, Kretschmannova et al, 2012). However, without specific receptor blockade and/or
522 genetic interventions (e.g. modification of ion channel expression level) these deductions
523 are largely speculative.
524
525 A recent study in the GH3 pituitary cell line has implicated NALCN as a major contributor
526 to the NSCC activity (Impheng et al, 2021). Therefore, we knockdown NALCN activity
527 and used sophisticated electrophysiology and calcium imaging to determine its role in
528 regulating cellular excitability and $[Ca^{2+}]_i$ oscillations in native anterior endocrine pituitary
529 cells. Remarkably, our results revealed that NALCN channel determines a major Na^+
530 leak conductance in these cells, and its activity is critical to sustaining spontaneous firing
531 activity. Our results also show that NALCN is the main contributor to the depolarising
532 NSCC conductance in pituitary cells, without which the cells remained hyperpolarised-
533 silent. In addition, we show that NALCN is crucial for maintaining spontaneous ($[Ca^{2+}]_i$)
534 oscillations in these cells, and is sensitive to extracellular Ca^{2+} level, as demonstrated
535 in neurons (Lu et al, 2010).
536
537 Indeed, we found that NALCN knockdown (KD) pituitary cells are significantly
538 hyperpolarised (by about 15 mV) compared to controls. Moreover, 90% of NALCN KD
539 pituitary cells were completely silent and lost the ability to generate action potential and
540 ($[Ca^{2+}]_i$) oscillations. Remarkably, restoring the NALCN-like conductance in NALCN KD
541 cells with dynamic clamp rescued cellular resting membrane potential (RMP) and firing
542 activity to normal level. By extension, the removal of such dynamic-clamp mimic of
543 NALCN conductance immediately returned the RMP to hyperpolarised state, silencing
544 the cells.
545
546 Together, these results revealed a critical role for NALCN in anterior endocrine pituitary
547 cells, both for maintaining spontaneous firing and ($[Ca^{2+}]_i$) oscillations.
548
549 **A small NALCN conductance sustains a large depolarising drive**
550 The comparison between background Na^+ inward current in control cells and NALCN KD
551 cells showed that the amount of NALCN conductance knocked down in our experiments
552 was about 0.03 nS. This is consistent with the median of 0.05 nS background Na^+
553 conductance required to reactivate silent NALCN KD cells with dynamic clamp. This
554 dynamic clamp-based estimate does not rely on measurements of small noisy currents
555 (a few pA) in voltage-clamp, and therefore provides an estimate that is not affected by
556 poor signal-to-noise ratio (Milescu et al, 2008). The profound effect on electrical activity
557 of such a small conductance is consistent with measurements of high input resistance in
558 pituitary cells, the order of 5 GΩ (Oxford and Dubinsky, 1988), where a very small

559 variation in the current results in a drastic change in RMP. Indeed, with a reversal
560 potential close to 0 mV for this conductance, at a membrane potential of -60 mV, the
561 current through a 0.05 nS NALCN conductance is 3 pA. Therefore, with a membrane
562 resistance of 5 GΩ, the depolarisation due to the current is 15 mV, a value that is
563 remarkably consistent with our finding that NALCN KD cells were hyperpolarised by ~
564 15 mV.
565
566 We have employed a knockdown approach that is similar to that used in GH3 cells
567 (Impheng et al, 2021), where an estimated NALCN conductance of about 30 pS/pF is
568 reported. This represents a conductance of about three times larger than our estimate in
569 native pituitary cells (10 pS/pF, given our average pituitary cell capacitance of 5 pF). This
570 discrepancy in conductance may be due to the fact that we used a slightly higher
571 extracellular concentration of Mg^{2+} than in Impheng et al, 2021 (1 mM vs 0.8 mM). Given
572 that divalent cations can block NALCN (Chua et al, 2020), this may in part explain the
573 differences seen. A limitation of our work is we have sampled from a heterogenous
574 population of pituitary cells. Thence, different cell-types may express different level of
575 NALCN. If such expression heterogeneity exists, then our estimate of NALCN
576 conductance is an aggregate of the average NALCN conductance expressed by the
577 various cells sampled. Another possibility is that GH3 cells may simply express higher
578 levels of NALCN than primary pituitary cells.
579
580 Notably, there is no available estimate for NALCN single-channel conductance in
581 pituitary cells. It is therefore likely that with such knockdown-based approach we are
582 slightly under-estimating NALCN conductance in NALCN KD cells, since there may still
583 be some residual channels expression/conductance. Nevertheless, our estimation of
584 0.05 nS for NALCN conductance implies a low level of active NALCN channel expression
585 in the the pituitary cell membrane. This may provide support and a parsimonious
586 explanation as to why in our recordings (Figure 4A, 6A), and in the recording of others
587 (Liang et al, 2011) the non-specific cation current is very noisy. Since NALCN has weak
588 voltage sensitivity (Bouasse et al, 2019, Chua et al, 2020) transient blockade by divalent
589 cations, and possibly random channel gating, would result in relatively large current
590 fluctuations if the number of channels is low.
591
592 **NALCN activity is modulated by extracellular Ca^{2+} in pituitary cells**
593 Our results also revealed that in mouse anterior pituitary cells, NALCN channels are
594 sensitive to low extracellular Ca^{2+} ($[Ca^{2+}]_e$), and mediate a low-$[Ca^{2+}]_e$-induced
595 membrane depolarisation. Consistent with this observation, an increase in $[Ca^{2+}]_e$
596 caused hyperpolarisation in cultured rat pituitary somatotrophs through mechanism that

597 does not involved calcium channels (Tsaneva-Atanasova et al, 2007). The $[Ca^{2+}]_e$-
598 evoked membrane excitation we observed agrees with work in cultured rat lactotrophs
599 and somatotrophs (Sankaranarayanan and Simasko, 1996; Tsaneva-Atanasova et al,
600 2007), but here we unequivocally revealed that NALCN is directly involved. Our result is
601 also consistent with observation in neurons (Lu et al, 2010; Chu et al, 2003; Bouasse et
602 al, 2019), and work reporting NALCN sensitivity to $[Ca^{2+}]_e$ blockade in GH3 cells
603 (Impheng et al, 2021).
604
605 Two different mechanisms have been proposed to underlie the $[Ca^{2+}]_e$ sensing capacity
606 of NALCN. First, this may occur through the Ca^{2+}-sensing receptor (CaSR) *via* a G_q-
607 protein dependent pathway that ultimately induces NALCN phosphorylation by protein
608 kinase C (Lu et al, 2010; Lee et al, 2019). Alternatively, NALCN $[Ca^{2+}]_e$ sensitivity could
609 emerge through direct Ca^{2+} binding within the NALCN pore (Chua et al, 2020). In our
610 experiments, the inward leak current in the majority of the pituitary cells started to
611 increase within 20 seconds after $[Ca^{2+}]_e$ removal and continued to increase for the next
612 few minutes until it reaches a plateaux (Figure 6A). Thus, although the exact
613 mechanism(s) involved in the NALCN sensing of $[Ca^{2+}]_e$ in primary pituitary cells is yet
614 to be determined, the timing we observed (with regards to the development of the inward
615 leak current to plateaux level) favours a transduction cascade mechanism over a direct
616 pore effect.
617
618 Under both physiological and pathological circumstances, $[Ca^{2+}]_e$ can drop markedly in
619 the brain and blood serum (Ren, 2011; Ferry et al, 1997). This variation in $[Ca^{2+}]_e$ is
620 closely linked with adrenocorticotropic hormone (ACTH) secretion from pituitary
621 corticotrophs (Isaac et al, 1984; Fuleihan et al, 1996). In addition, physiological range
622 variations in serum Ca^{2+} is associated with drastic changes in ACTH secretion (Isaac et
623 al, 1984; Fuleihan et al, 1996). Our results, therefore, provide a plausible mechanism for
624 $[Ca^{2+}]_e$ sensing in pituitary cells, and link this with appropriate hormonal secretion under
625 normal and pathological states.
626
627 **NALCN modulation by neurohormones: a likely key player in pituitary cell**
628 **responses to hypothalamic/feedback signals?**
629 Our finding that NALCN activity has a profound effect on pituitary cell excitability raises
630 the possibility that beyond extracellular Ca^{2+} sensing, NALCN could potentially provide
631 a highly sensitive signalling conduit/target through which hypothalamic
632 neurochemicals/neurohormones could act to regulate hormonal function.
633 In support, NALCN can be regulated by G-protein dependent and independent signalling
634 pathways (Lu et al, 2009; Swayne et al, 2009; Philippart & Khaliq, 2018), providing a

635 possible intracellular access to its activity by a multitude of receptor systems. Moreover,
636 NALCN is sensitive to hypothalamic neuropeptides, such as Substance P and
637 neurotensin (Lu et al, 2009) which activity have been linked with hormonal regulation
638 (Eckstein et al, 1980). In GH3 cells, NALCN activity promotes basal and TRH-dependent
639 prolactin secretion (Impheng et al, 2021).
640
641 These observations are consistent with other *in vitro* work showing that the removal of
642 extracellular Na^+ to suppress NSCC activity (which our data now identifies as primarily
643 NALCN-driven) in rat pituitary cells negates the ability for growth hormone releasing
644 hormone (GHRH) to evoke growth hormone secretion from these cells (Kato et al, 1988),
645 mostly by preventing (GHRH)-induced Ca^{2+} influx (Lussier et al, 1991; Naumov et al,
646 1994). This suppression in hormonal secretion is TTX-insensitive and can be rescued by
647 RMP depolarisation with artificially high extracellular K^+ (Kato et al, 1988). This supports
648 that a Na^+-dependent depolarising mechanism other than TTX-sensitive voltage-gated
649 Na^+ channels indeed operates to sensitised hormonal-dependent hormone release by
650 pituitary cells.
651
652 Removal of extracellular Na^+ in murine corticotroph cells also substantially delayed the
653 stimulatory response of these cells to corticotrophin-releasing hormone (CRH) (Liang et
654 al, 2011), presumably by suppressing spontaneous $[Ca^{2+}]_i$ oscillations in the cells (Tomić
655 et al, 2011). In addition, progesterone and oestrogen have been shown to regulate
656 NALCN expression in human myometrial cells (Amazu et al, 2020), although this remains
657 to be determined in the pituitary. Therefore, altogether, this raises the possibility that
658 hormones and neuropeptides may modulate pituitary NALCN activity in a multifaceted
659 fashion and timescale to influence hormonal release.
660
661 In summary, our targeted NALCN knockdown approach, electrophysiology, and calcium
662 imaging methods have highlighted the importance of NALCN activity in supporting
663 appropriate excitability in native pituitary cells. This uncovering may provide an important
664 step in our understanding of pituitary cells excitability and its intersection with hormonal
665 regulation. It may also provide a potential target for therapeutic interventions in
666 endocrine-related disorders that are linked with disruptions in pituitary hormone
667 secretion.
668
669
670
671
672

673 **Materials and Methods**

674

675 **Primary cell culture**

676 Murine endocrine anterior pituitary cell cultures were prepared between 8:00 and 11:00
677 AM from wild-type C57BL/6J mice as required. Mice were kept in groups of two to four
678 under standard circumstances at the University of Exeter (UK) animal unit: Lights on at
679 6:00 AM, lights off at 6:00 PM at 21°C, tap water and food were available *ad libitum*. The
680 adult mice aged between two to six months were selected randomly regardless of their
681 sex. All the animal work was carried out according to the standards of the Home Office
682 (England) and the University of Exeter. Three or four mice were culled via cervical
683 dislocation and then were decapitated in accordance with Schedule 1 procedures. After
684 removing the brain, the pituitary gland was removed from the sella turcica (bony cavity)
685 and placed in a 100x21 mm culture dish (Thermo Fisher Scientific, UK) containing 150
686 µL 4°C DMEM (Dulbecco's modified Eagle's medium with high glucose and 25mM
687 HEPES from Sigma Aldrich (Merck), UK) located on ice. Under a dissection microscope,
688 the intermediate and posterior lobes were removed using a scalpel blade (size 10), and
689 the anterior lobes were chopped to small pieces manually. Subsequently, the chopped
690 tissues were transferred into a 50 mL falcon tube containing 2.5 mL DMEM
691 supplemented with 207 TAME Units/mL trypsin and 36 Kunitz Units/mL DNase I (both
692 from Sigma Aldrich, UK), and then incubated in 37°C water bath for 10 minutes. Every 5
693 minutes, the tube was swirled to disperse the tissue pieces evenly to achieve a thorough
694 digestion. After 10 minutes, the suspension was gently triturated 20-30 times using a 1
695 mL pipette tip. At the end of the digestion step, an inhibition solution containing 5 mL
696 DMEM supplemented with 0.25 mg/mL Lima soybean trypsin inhibitor, 100 kallikrein unit
697 aprotinin and 36 Kunitz Units/ml DNase I (Sigma Aldrich, UK) was added to the digestion
698 solution, and the cell suspension was left for a few minutes to inactivate the trypsin
699 enzyme activity. The resulting suspension was finally filtered through a cell strainer with
700 70 µm nylon mesh (Merck) and was centrifuged at 100×g for 10 minutes. The pellet was
701 resuspended in 500-600 µL DMEM solution and then 60 µL was plated on each 15 mm
702 diameter round coverslip (Thermo Fisher Scientific, UK) in a 12-well plate. After 20
703 minutes, once the cells were securely attached to the bottom of coverslips, 1 mL of
704 growth medium (DMEM + 2.5% FBS + 0.1 % Fibronectin + 1% antibiotic-penstrep, from
705 Sigma Aldrich, UK) was added to each well and then incubated at 37°C in a 5% CO_2
706 incubator. The culture medium was replaced with antibiotic-free growth-medium 6 hours
707 later. The growth medium was refreshed every two days. 5 µL concentrated suspension
708 of lentivirus was added to the medium in each well of a 12-well plate. Fresh growth
709 medium was substituted 24 hours after transduction. Green fluorescence cells were
710 usually observable 2-3 days after transduction and selected for electrophysiological

711 recording. Each batch of primary pituitary cell culture was utilized for up to 5 days after
712 transduction for electrophysiological recordings and calcium imaging.
713
714 **Lentivirus**
715 A microRNA-adapted shRNA based on miR-30 for specific NALCN silencing cloned in
716 the lentiviral pGIPZ plasmid and targeting the 5'-GCAACAGACTGTGGCAATT-3' region
717 of the rat NALCN-encoding RNA was obtained from a commercial source (Dharmacon
718 #V2LMM_90196). A non-silencing scramble control was used in our experiments
719 (Dharmacon #RHS4346). HpaI/BamHI are the restriction sites in pGIPZ plasmid
720 between which the NALCN silencing shRNA was inserted.
721
722 **Electrophysiological recording**
723 Electrophysiological recordings from pituitary cells were performed at room temperature
724 using single-cell amphotericin-perforated patch-clamp technique. The recordings were
725 obtained using an Axopatch 700B amplifier and Clampex 10.1 (Molecular Devices) with
726 a sampling rate of 10 kHz and filtered at 2 kHz (lower pass). Patch pipettes were
727 fabricated from borosilicate glass with filament (outer diameter: 1.50 mm and inner
728 diameter: 0.86 mm, Warner Instrument-multi channel system distributer) and pulled
729 using a micropipette puller (Sutter Instruments, model P-97). Pipette tips were then fire
730 polished and had a resistance ranging from 4 to 6 MΩ. Once a high resistance seal was
731 formed (>10 GΩ), usually within 10 minutes of patching, the access resistance (or series
732 resistance) would reduce to less than 50 MΩ, and then recording started. If the seal
733 resistance was less than 10 GΩ, the cell was discarded. In current clamp mode, series
734 resistance was compensated by Bridge-Balance and was usually less than 40 MΩ.
735 Junction potential was not corrected. In voltage clamp mode, compensated series
736 resistance (60%) was normally less than 50 MΩ and the capacitance of recorded pituitary
737 cells ranged between 4 and 6 pF (electronic compensation was done *via* whole-cell mode
738 of multiclamp 700B). During recording, the cells were constantly perfused using a gravity-
739 driven perfusion system, with a flow rate of 0.5 mL/min with extracellular solution
740 containing (in millimolar) 138 NaCl, 5 KCl, 10 alpha-D-glucose, 25 HEPES, 0.7 Na_2HPO_4,
741 1 $MgCl_2$ and 2 $CaCl_2$. The pH was adjusted to 7.4 with NaOH, and the osmolality was
742 305 mOsmol/L. Patch pipettes were filled with an intracellular solution containing (in
743 millimolar) 10 NaCl, 100 K-Gluconate, 50 KCl, 10 HEPES, and 1 $MgCl_2$. The pH was
744 adjusted to 7.2 with KOH, 295 mOsmol/L. The osmolality of the solutions was maintained
745 by adding an inert ingredient sucrose. 5 µl Amphotericin-B of a stock solution (20 mg/mL
746 in dimethyl sulfoxide) was added to 1 mL of pipette solution to achieve a final
747 concentration of 50 µg/ml. Other concentrations such as 10 µl Amphotericin-B were also

748 tried, however 5 µl resulted in more durability of the recording (all salts and Amphotericin-
749 B were purchased from Sigma Aldrich.
750
751 **Dynamic clamp**
752 With dynamic clamp we can effectively change the biophysical property of ion channels
753 (such as activation, inactivation, gating kinetics and conductances) as we choose and
754 investigate how these manipulations affect the pattern of electrical activity in real time.
755 In other words, we can establish the contribution of a type of ion channel to regulating
756 various aspects of electrical activity (Milescu et al, 2008).
757
758 In this study, a second computer and an analogue-to-digital acquisition card (DAQ,
759 National Instruments) were installed to run the dynamic clamp module in the software
760 QuB (Milescu et al, 2008). In the current clamp mode of the Axopatch 700B amplifier,
761 the membrane potential (Vm) of a patched cell was recorded in real time and passed to
762 the computer running QuB as an input for a mathematical expression of non-selective
763 cationic leak channels: $I_{NS}=g_{NS}$ (Vm - E_{NS}) which defines the corresponding current (I_{NS})
764 going through them. The sodium leak conductance (g_{NS}) was changed manually. The
765 calculated I_{NS} was then injected back to the cell via the same DAQ and then the
766 membrane voltage response was recorded. Thus, the injected NALCN-like current is
767 varied dynamically, unlike conventional current clamp in which the injected current is
768 constant across all time points.
769
770 The reversal potential (E_{NS}) for this channel was considered zero since this channel is
771 permeable to different monovalent cations (e.g. K^+ and Na^+) but primarily to Na^+ (Lu et
772 al, 2007; Chua et al, 2020).
773
774 **Measurement of cytosolic calcium in single pituitary cells**
775 The coverslips with pituitary cells were bathed in the extracellular solution (containing
776 same ingredients as described in the above electrophysiology section) with 2µM fura-2
777 AM (Thermo Fischer Scientific-# F1221) for 45 minutes at 37°C. The cells were then
778 rinsed three times with the extracellular solution using a 2 mL Pasteur pipette. Following
779 this, the coverslips were mounted onto the recording chamber (volume ~ 0.2 mL) on the
780 stage of an inverted microscope (Nikon eclipse Ti). Cells were constantly perfused with
781 the extracellular solution at room temperature using a gravity-driven perfusion system.
782 Cells were excited every 1 second with alternating 340-nm and 380-nm light beams (20
783 millisecond exposure time) originating from a Lambda DG-4 wavelength switcher (Sutter
784 Instrument Company). Light intensity was reduced by 50% before hitting the cells using
785 an appropriate filter. The intensity of emitted light was measured at 520 nm and images

786 were acquired by a Hamamatsu digital camera C1344 set to 4 × 4 binning. Hardware
787 control was achieved by TI Workbench software developed by T. Inoue (Tabak et al,
788 2010). Using this software, regions of interest (ROI) were selected around the cells that
789 were not overlapping with other cells and a single background ROI was selected in an
790 empty space. Pixel values within each region of interest were averaged for both 340 and
791 380 excitation wavelengths and then subtracted from the background. Following this, a
792 ratio (*r)* was computed according to the formula:
793 $r = (ROI_{340} - ROI_{background340})/ (ROI_{380} - ROI_{background380})$
794 Trace analysis was performed in MATLAB.
795
796 **Immunohistochemistry**
797 Pituitary glands were extracted and fixed overnight in 4% PFA in PBS. The following day,
798 70 µm thick sections were cut using a vibratome (Campden Instruments, UK), placed on
799 poly-L-Lysine coated microscope slides (VWR) and left to dry. Next, the sections were
800 blocked with 10% FBS in PBST (PBS containing 0.01% Triton X-100) for one hour at
801 room temperature. Primary rabbit anti-NALCN antibody at 1:500 dilution (Alomone Labs,
802 Israel, #ASC-022) in 10% FBS/PBST was applied to the sections and incubated in humid
803 chamber at 4 C° degrees overnight. The next day, sections were washed 3 times for 15
804 min with PBST. Then, the secondary 488-Alexa-Fluor conjugated antibody (at 1:1000,
805 Molecular Probes) was applied in 10% FBS/PBST solution for 1 hour at room
806 temperature, followed by a series of three 15 min washes with PBST. The nucleic acids
807 present in the pituitary gland cells were visualised with TOTO-3 (1:2000, Thermo Fisher
808 Scientific). Sections were incubated with TOTO-3 for 15 min on an agitated surface, then
809 washed three times (each time 10 min) and subsequently mounted with Fluorsave
810 medium (Calbiochem). The controls were the sections where primary antibody was
811 omitted. Images were obtained using a Zeiss LSM 5 Exciter confocal microscope run by
812 Zen software.
813
814
815 **Statistics**
816 We use MATLAB for all statistical analysis and the type of statistical test used in each
817 case is specified in the results.
818
819 **Acknowledgements**
820 We would like to thank the members of the University of Exeter Biological Services Unit
821 for their assistance in colony maintenance and husbandry. This work was funded by the
822 University of Exeter PhD studentship to MB, Wellcome Trust ISSF award to JT and JJW,
823 and grant from the Biotechnology and Biological Sciences Research Council (BBSRC)

824 to MDCB (BB/S01764X/1). JJW also acknowledges financial support from the Medical
825 Research Council (MR/N008936/1).

826

827 **References**

828 Amazu, C., Ma, X., Henkes, C., Ferreira, J., Santi, C., & England, S., 2020. Progesterone
829 and estrogen regulate NALCN expression in human myometrial smooth muscle
830 cells. American Journal Of Physiology-Endocrinology And Metabolism, 318, E441-E452.
831 https://doi.org/10.1152/ajpendo.00320.2019
832
833 Bertram, R., Satin, L.S., Sherman, A.S., 2018. Closing in on the Mechanisms of Pulsatile
834 Insulin Secretion. Diabetes 67, 351–359. https://doi.org/10.2337/dbi17-0004

835 Bouasse, M., Impheng, H., Servant, Z., Lory, P., Monteil, A., 2019. Functional expression
836 of CLIFAHDD and IHPRF pathogenic variants of the NALCN channel in neuronal cells
837 reveals both gain- and loss-of-function properties. Sci. Rep. 9, 11791.
838 https://doi.org/10.1038/s41598-019-48071-x

839 Chu, X., Zhu, X., Wei, W., Li, G., Simon, R.P., MacDonald, J.F., Xiong, Z., 2003. Acidosis
840 decreases low Ca^{2+} -induced neuronal excitation by inhibiting the activity of calcium-
841 sensing cation channels in cultured mouse hippocampal neurons. J. Physiol. 550, 385–
842 399. https://doi.org/10.1113/jphysiol.2003.043091

843 Chua, H.C., Wulf, M., Weidling, C., Rasmussen, L.P., Pless, S.A., 2020. The NALCN
844 channel complex is voltage sensitive and directly modulated by extracellular calcium.
845 Sci. Adv. 6, eaaz3154. https://doi.org/10.1126/sciadv.aaz3154

846 Cui, Y., Kam, K., Sherman, D., Janczewski, W.A., Zheng, Y., Feldman, J.L., 2016.
847 Defining preBötzinger Complex Rhythm- and Pattern-Generating Neural Microcircuits In
848 Vivo. Neuron 91, 602–614. https://doi.org/10.1016/j.neuron.2016.07.003

849 Eckstein, N., Wehrenberg, W., Louis, K., Carmel, P., Zimmermann, E., Frantz, A., &
850 Ferin, M., 1980. Effects of Substance P on Anterior Pituitary Secretion in the Female
851 Rhesus Monkey. Neuroendocrinology, 31, 338-342. https://doi.org/10.1159/000123098

852 Ferry, S., Chatel, B., Dodd, R.H., Lair, C., Gully, D., Maffrand, J.-P., Ruat, M., 1997.
853 Effects of Divalent Cations and of a Calcimimetic on Adrenocorticotropic Hormone
854 Release in Pituitary Tumor Cells. Biochem. Biophys. Res. Commun. 238, 866–873.
855 https://doi.org/10.1006/bbrc.1997.7401

856 Fletcher, P.A., Sherman, A., Stojilkovic, S.S., 2018. Common and diverse elements of
857 ion channels and receptors underlying electrical activity in endocrine pituitary cells. Mol.
858 Cell. Endocrinol. 463, 23–36. https://doi.org/10.1016/j.mce.2017.06.022

859 Flourakis, M., Kula-Eversole, E., Hutchison, A.L., Han, T.H., Aranda, K., Moose, D.L.,
860 White, K.P., Dinner, A.R., Lear, B.C., Ren, D., Diekman, C.O., Raman, I.M., Allada, R.,
861 2015. A Conserved Bicycle Model for Circadian Clock Control of Membrane Excitability.
862 Cell 162, 836–848. https://doi.org/10.1016/j.cell.2015.07.036

863 Fuleihan, G.E., Brown, E.M., Gleason, R., Scott, J., Adler, G.K., 1996. Calcium
864 modulation of adrenocorticotropin levels in women--a clinical research center study. J.
865 Clin. Endocrinol. Metab. 81, 932–936. https://doi.org/10.1210/jcem.81.3.8772553

866 Impheng, H., Lemmers, C., Bouasse, M., Legros, C., Pakaprot, N., Guérineau, N.C.,
867 Lory, P., Monteil, A., 2021. The sodium leak channel NALCN regulates cell excitability of
868 pituitary endocrine cells. FASEB J. 35. https://doi.org/10.1096/fj.202000841RR

869 Isaac, R., Raymond, J.-P., Rainfray, M., Ardaillou, R., 1984. Effects of an acute calcium
870 load on plasma ACTH, cortisol, aldosterone and renin activity in man. Acta Endocrinol.
871 (Copenh.) 105, 251–257. https://doi.org/10.1530/acta.0.1050251

872 Kato, M., Hattori, M.A., Suzuki, M., 1988. Inhibition by extracellular Na^+ replacement of
873 GRF-induced GH secretion from rat pituitary cells. Am. J. Physiol.-Endocrinol. Metab.
874 254, E476–E481. https://doi.org/10.1152/ajpendo.1988.254.4.E476

875 Kayano, T., Sasaki, Y., Kitamura, N., Harayama, N., Moriya, T., Dayanithi, G.,
876 Verkhratsky, A., Shibuya, I., 2019. Persistent Na+ influx drives L-type channel resting
877 Ca2+ entry in rat melanotrophs. Cell Calcium 79, 11–19.
878 https://doi.org/10.1016/j.ceca.2019.02.001

879 Kretschmannova, K., Kucka, M., Gonzalez-Iglesias, A.E., Stojilkovic, S.S., 2012. The
880 Expression and Role of Hyperpolarization-Activated and Cyclic Nucleotide-Gated
881 Channels in Endocrine Anterior Pituitary Cells. Mol. Endocrinol. 26, 153–164.
882 https://doi.org/10.1210/me.2011-1207

883 Kucka, M., Kretschmannova, K., Murano, T., Wu, C.-P., Zemkova, H., Ambudkar, S.V.,
884 Stojilkovic, S.S., 2010. Dependence of Multidrug Resistance Protein-Mediated Cyclic
885 Nucleotide Efflux on the Background Sodium Conductance. Mol. Pharmacol. 77, 270–
886 279. https://doi.org/10.1124/mol.109.059386

887 Kučka, M., Kretschmannová, K., Stojilkovic, S.S., Zemková, H., Tomić, M., 2012.
888 Dependence of Spontaneous Electrical Activity and Basal Prolactin Release on
889 Nonselective Cation Channels in Pituitary Lactotrophs. Physiol. Res. 267–275.
890 https://doi.org/10.33549/physiolres.932301

891 Kwiecien, R., Hammond, C., 1998. Differential Management of Ca^{2+} Oscillations by
892 Anterior Pituitary Cells: A Comparative Overview. Neuroendocrinology 68, 135–151.
893 https://doi.org/10.1159/000054360

894 Lee, S.-Y., Vuong, T.A., Wen, X., Jeong, H.-J., So, H.-K., Kwon, I., Kang, J.-S., Cho, H.,
895 2019. Methylation determines the extracellular calcium sensitivity of the leak channel
896 NALCN in hippocampal dentate granule cells. Exp. Mol. Med. 51, 1–14.
897 https://doi.org/10.1038/s12276-019-0325-0

898 Liang, Z., Chen, L., McClafferty, H., Lukowski, R., MacGregor, D., King, J.T., Rizzi, S.,
899 Sausbier, M., McCobb, D.P., Knaus, H., Ruth, P., Shipston, M.J., 2011. Control of
900 hypothalamic–pituitary–adrenal stress axis activity by the intermediate conductance
901 calcium-activated potassium channel, SK4. J. Physiol. 589, 5965–5986.
902 https://doi.org/10.1113/jphysiol.2011.219378

903 Lu, B., Su, Y., Das, S., Liu, J., Xia, J., Ren, D., 2007. The Neuronal Channel NALCN
904 Contributes Resting Sodium Permeability and Is Required for Normal Respiratory
905 Rhythm. Cell 129, 371–383. https://doi.org/10.1016/j.cell.2007.02.041

906 Lu, B., Zhang, Q., Wang, H., Wang, Y., Nakayama, M., Ren, D., 2010. Extracellular
907 Calcium Controls Background Current and Neuronal Excitability via an UNC79-UNC80-

NALCN Cation Channel Complex. Neuron 68, 488–499. https://doi.org/10.1016/j.neuron.2010.09.014

Lussier, B.T., French, M.B., Moor, B.C., Kraicer, J., 1991. Free Intracellular Ca2+ Concentration and Growth Hormone (GH) Release from Purified Rat Somatotrophs, III. Mechanism of Action of GH-Releasing Factor and Somatostatin*. Endocrinology 128, 592–603. https://doi.org/10.1210/endo-128-1-592

Lutas, A., Lahmann, C., Soumillon, M., Yellen, G., 2016. The leak channel NALCN controls tonic firing and glycolytic sensitivity of substantia nigra pars reticulata neurons. eLife 5, e15271. https://doi.org/10.7554/eLife.15271

Mollard, P., Schlegel, W., 1996. Why are endocrine pituitary cells excitable? Trends Endocrinol. Metab. 7, 361–365. https://doi.org/10.1016/S1043-2760(96)00186-5

Naumov, A.P., Herrington, J., Hille, B., 1994. Actions of growth-hormone-releasing hormone on rat pituitary cells: intracellular calcium and ionic currents. Pflugers Arch. Eur. J. Physiol. 427, 414–421. https://doi.org/10.1007/BF00374255

Philippart, F., Khaliq, Z.M., 2018. Gi/o protein-coupled receptors in dopamine neurons inhibit the sodium leak channel NALCN. eLife 7, e40984. https://doi.org/10.7554/eLife.40984

Protze, S.I., Liu, J., Nussinovitch, U., Ohana, L., Backx, P.H., Gepstein, L., Keller, G.M., 2017. Sinoatrial node cardiomyocytes derived from human pluripotent cells function as a biological pacemaker. Nat. Biotechnol. 35, 56–68. https://doi.org/10.1038/nbt.3745

Ren, D., 2011. Sodium Leak Channels in Neuronal Excitability and Rhythmic Behaviors. Neuron 72, 899–911. https://doi.org/10.1016/j.neuron.2011.12.007

Rorsman, P., Ashcroft, F.M., 2018. Pancreatic β-Cell Electrical Activity and Insulin Secretion: Of Mice and Men. Physiol. Rev. 98, 117–214. https://doi.org/10.1152/physrev.00008.2017

Sankaranarayanan, S., Simasko, S.M., 1996. A role for a background sodium current in spontaneous action potentials and secretion from rat lactotrophs. Am. J. Physiol.-Cell Physiol. 271, C1927–C1934. https://doi.org/10.1152/ajpcell.1996.271.6.C1927

Shi, Y., Abe, C., Holloway, B.B., Shu, S., Kumar, N.N., Weaver, J.L., Sen, J., Perez-Reyes, E., Stornetta, R.L., Guyenet, P.G., Bayliss, D.A., 2016. Nalcn Is a “Leak” Sodium Channel That Regulates Excitability of Brainstem Chemosensory Neurons and Breathing. J. Neurosci. 36, 8174–8187. https://doi.org/10.1523/JNEUROSCI.1096-16.2016

Simasko, S.M., 1994. A background sodium conductance is necessary for spontaneous depolarizations in rat pituitary cell line GH3. Am. J. Physiol.-Cell Physiol. 266, C709–C719. https://doi.org/10.1152/ajpcell.1994.266.3.C709

Stojilkovic, S.S., 2006. Pituitary cell type-specific electrical activity, calcium signaling and secretion. Biol. Res. 39. https://doi.org/10.4067/S0716-97602006000300004

Stojilkovic, S.S., Kretschmannova, K., Tomić, M., Stratakis, C.A., 2012. Dependence of the Excitability of Pituitary Cells on Cyclic Nucleotides: Cyclic nucleotides and excitability of pituitary cells. J. Neuroendocrinol. 24, 1183–1200. https://doi.org/10.1111/j.1365-2826.2012.02335.x

Stojilkovic, S.S., Tabak, J., Bertram, R., 2010. Ion Channels and Signaling in the Pituitary Gland. Endocr. Rev. 31, 845–915. https://doi.org/10.1210/er.2010-0005

Stojilkovic, S.S., Zemkova, H., Van Goor, F., 2005. Biophysical basis of pituitary cell type-specific Ca2+ signaling–secretion coupling. Trends Endocrinol. Metab. 16, 152–159. https://doi.org/10.1016/j.tem.2005.03.003

Swayne, L.A., Mezghrani, A., Varrault, A., Chemin, J., Bertrand, G., Dalle, S., Bourinet, E., Lory, P., Miller, R.J., Nargeot, J., Monteil, A., 2009. The NALCN ion channel is activated by M3 muscarinic receptors in a pancreatic β-cell line. EMBO Rep. 10, 873–880. https://doi.org/10.1038/embor.2009.125

Tomić, M., Kucka, M., Kretschmannova, K., Li, S., Nesterova, M., Stratakis, C.A., Stojilkovic, S.S., 2011. Role of nonselective cation channels in spontaneous and protein kinase A-stimulated calcium signaling in pituitary cells. Am. J. Physiol.-Endocrinol. Metab. 301, E370–E379. https://doi.org/10.1152/ajpendo.00130.2011

Tsaneva-Atanasova, K., Sherman, A., van Goor, F., Stojilkovic, S.S., 2007. Mechanism of Spontaneous and Receptor-Controlled Electrical Activity in Pituitary Somatotrophs: Experiments and Theory. J. Neurophysiol. 98, 131–144. https://doi.org/10.1152/jn.00872.2006

Vela, J., Pérez-Millán, M.I., Becu-Villalobos, D., Díaz-Torga, G., 2007. Different kinases regulate activation of voltage-dependent calcium channels by depolarization in GH3 cells. Am. J. Physiol.-Cell Physiol. 293, C951–C959. https://doi.org/10.1152/ajpcell.00429.2006

Yeh, S.-Y., Huang, W.-H., Wang, W., Ward, C.S., Chao, E.S., Wu, Z., Tang, B., Tang, J., Sun, J.J., Esther van der Heijden, M., Gray, P.A., Xue, M., Ray, R.S., Ren, D., Zoghbi, H.Y., 2017. Respiratory Network Stability and Modulatory Response to Substance P Require Nalcn. Neuron 94, 294-303.e4. https://doi.org/10.1016/j.neuron.2017.03.024

Zemkova, H., Tomić, M., Kucka, M., Aguilera, G., Stojilkovic, S.S., 2016. Spontaneous and CRH-Induced Excitability and Calcium Signaling in Mice Corticotrophs Involves Sodium, Calcium, and Cation-Conducting Channels. Endocrinology 157, 1576–1589. https://doi.org/10.1210/en.2015-1899